Parameter Scaling Protocol for Upper-limb Musculoskeletal Models

Pablo Peñas

Technische Universiteit Delft, Delft, The Netherlands

Abstract

Generic musculoskeletal models are not reliable predicting inter-individual variations in muscle forces. Scaling the model parameters is necessary to represent the muscle characteristics of the subjects and thus to pinpoint the differences in force capacity. Optimal Fiber (OFL) and Tendon Slack Length (TSL) have been identified as the two most influential parameters in muscle force generation. The goal of the current study is adjusting a lower-limb scaling algorithm for OFL and TSL to the Delft Shoulder and Elbow Model (DSEM). Furthermore, we evaluate the effect on the preservation of model consistency and muscle force production. Firstly, we scaled the DSEM geometrically. That drove twenty-two muscles to work out of the physiological range in the F-L curve up to 41% of the shoulder ROM. Moreover, the consistency of the model dropped by 78%. We tested three approaches to scale OFL and TSL. The constrained method delivered the best results reducing these percentages to 8% and 2.9%, respectively. It also increased the muscle force production of the DSEM 1.2%BW compared to the geometrically scaled version. The adaptation of the constrained scaling algorithm to the DSEM provides consistency values in the same range observed in lower-limb models. Therefore, we state that it is necessary to scale OFL and TSL whenever the dimensions of the DSEM are modified to obtain reliable muscle force estimations. We recommend further validation of the procedure developed in this article, for example, against data from instrumented endoprosthesis.

Keywords: Musculoskeletal Model, Delft Shoulder and Elbow Model, Optimal Fiber Length, Tendon Slack Length, Scaling, Upper-limb, Muscle-tendon parameters

1. Introduction

Musculoskeletal (MSK) models provide a unique insight into aspects of the internal functioning of the locomotive system, such as net joint moments and muscle forces. Their initial purpose was raising knowledge about the bases of the MSK system. Early studies cover topics such as muscle collaboration to produce torques around joints [1], and estimation of the differences in joint loading during diverse tasks [2, 3]. In recent years, MSK models start to be helpful as well in the clinical field. Modern studies use them to predict the outcomes of tendon transfer surgeries [4] ("what if" simulations) and to explain how neuromuscular pathologies alter motion [5, 6].

Generic models, created from cadaveric data, are suitable for first-time investigations because they analyze the loading changes among tasks, not individuals. However, generic models are not appropriate for contemporary researches. These studies focus on the variations in muscle force capacity among subjects (instead of tasks), and models employing cadaveric data do not account for those differences [7]. In this landscape, MSK models should be capable of reproducing the force capability of the subjects. Hence, the set of parameters that determines the generation of force in MSK models must be scaled accordingly to the anatomical characteristics of the individuals [8, 9, 10, 11].

There are three groups of parameters in MSK models: geometrical, inertial, and muscle. Medical imaging, like MRI and CT-scans, allows measuring geometrical (for instance, segment dimensions and musculotendon lengths) [12], inertial (segmental mass) [13], and some muscle parameters (Physiological Cross-Section Area) [14] in living subjects. No current techniques allow measuring other muscle parameters, such as optimal fiber (OFL) and tendon slack length (TSL), in-vivo and hence, it is troublesome to scale them. However, these last two parameters are the most influential of all of them for muscle force generation. Therefore the adjustment of OFL and TSL is essential for the MSK model to match the force capacity of the subject [15, 16].

Geometrical scaling is the first step to modify the cadaveric parameters of the model. It involves adjusting the dimensions of the segments and the calculation of the joints' center of rotation. The length of the musculotendon units (MTU) is scaled proportionally to preserve the direction of their

force vectors. Then, the segment mass is scaled accordingly to the whole body mass of the subject [17]. Several studies demonstrate that adjusting these parameters improves joint loading estimations [7, 18]. However, others shows that this level of scaling is not enough for a MSK model to represent the muscle force capacity of a subject [19, 11, 20]. Even though the next step seems to be modifying the muscle parameters of the model, it is not a common practice, given the reasons in the previous paragraph. The alternative is not adjusting OFL and TSL to the new MTUs length, which causes a shift in their working area in the Force-Length curve.

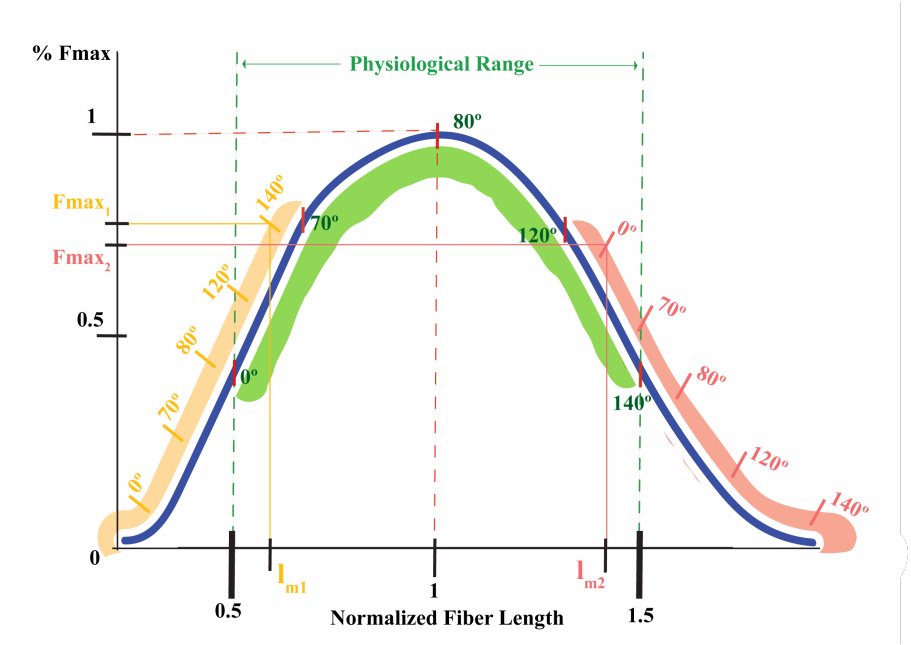

Figure 1: The coloured areas (yellow and red) shows the shift in the working area of an upper-limb muscle caused by modifying its length without accordingly adjusting its muscle parameters. The green area represents the length excursion of the muscle in the reference model (GM). F_{max1} and F_{max2} illustrate the decrease in muscle force production (both values are below the $F_{max} = 1$). Furthermore, the behavior of the muscle is altered since F_{max1} and F_{max2} do not take place at the optimal fiber length ($L^m_{norm} = 1$) but at $l_{m,norm1}$ and $l_{m,norm2}$. The degrees marked along each of the three zones illustrate the humeral elevation angle. It also shows how the altered muscle behavior affects the force production since for a certain angle (e.g., 120°) the force generated in each situation varies. The X-axis indicates the normalized fiber length, which is the ratio between the length of the muscle and its optimal fiber length (Eq. 9).

The F-L curve defines the maximum force a muscle can generate depending on its length. Figure 1 illustrates the F-L relation of a generic upper-limb muscle (in blue). In a generic model, all the muscles work within the physiological range (in green). However, the shift in the operating area caused by not adjusting the muscle parameters to the new MTUs length brings them to work out of the physiological area (red and yellow regions). In that situation, the force generation of the muscles decreases, and their force peak happens at a different angle of humeral elevation. Winby describes this event as a loss of consistency in the scaled model. He establishes that the aim of any scaling technique should be not altering the F-L working region of the MTUs of the model [21]. In other words, the goal must be preserving the consistency of the model. Otherwise, the scaling process provokes a loss in the force capacity of the muscles due to the shift in its working region which, ultimately, alters their behavior.

The literature on scaling muscle parameters for lower-limb models is quite extensive. A significant number of articles with different approaches have been published, which are classified on anthropometric or functional. The former rely solely on anatomical data [22, 21], while the later also employ dynamometry [23] or EMG [24, 10, 25]. Further studies have evaluated the influence of muscle parameters on the MTU moments in gait analyses [26, 16]. Nevertheless, all these experiments (as well as Winby's research) have only been conducted with lower-limb models, and literature on the topic for upper-limb models is very limited [27, 14, 28].

In conclusion, scaling the parameters of MSK models is essential to match the force capacity of a subject. The most common scaling approaches (geometrical techniques), however, provoke a loss of consistency in the scaled models. Consequently, these models do not match the force capability of the subjects. Studies involving lower-limb models have demonstrated that the loss of consistency is due to not scaling OFL and TSL [15, 16, 26]. Regarding upper-limb models however, no study has examined that, despite some articles having reported that geometrically scaled upper-limb models also underestimate muscle forces.[19]

The aim of this paper is studying the effect of scaling optimal fiber and tendon slack length on the consistency of geometrically scaled upper-limb models. We choose to adjust these two parameters following the recom-

mendations identified in the literature: maintain the model consistency and establish a non-linear relation between muscle length and OFL and TSL [15, 16, 8, 29]. For that purpose, we find the optimization algorithm developed by Modenese the best option available [22]. The first condition is that the optimization algorithm scales OFL and TSL at least. Secondly, it should be not need dynamometer or EMG measurements since these methods are computationally expensive and require extremely large quantities of data. As far as we know, the only approach with those characteristics and which is suitable for upper-limb models is Modenese's algorithm, although he did not prove it. Furthermore, his method outperforms the techniques reviewed by Winby in terms of preserving consistency, and contains a non-linear approach.

We hypothesized that adjusting OFL and TSL in geometrically scaled upper-limb models would enhance their consistency. Furthermore, we expected that improving the model's consistency would cause an increase in its muscle force production.

2. Materials and Methods

2.1. ***Musculoskeletal Model. The Delft Shoulder and Elbow Model.***

The Delft Shoulder and Elbow Model (DSEM) is a finite element model created by Van der Helm [30]. It depicts the upper-limb with six rigid bodies and thirty-one muscles, which divided in 139 contractile elements operate seventeen Degrees of Freedom (DOF). We named this version of the model the Generic Model (GM) [19].

We also employed the geometrically scaled models from Bolsterlee's investigation [14]. These are versions of the DSEM whose segments' length and mass were adjusted linearly according to the dimensions of five participants. The length of the contractile elements in these models also changed proportionally with the new segments' measures. The position of the glenohumeral center of rotation was calculated using instantaneous helical axes (IHA) [31]. Nevertheless, out of the five scaled subjects, only two of them completed the Inverse Kinematic (IK) analysis. In the other three, the simulation crashed due to a collision between the scapular and thoracic segments. Since the scapula, clavicle and thorax were modeled as a closed kinematic

chain, not every combination of joint angles is feasible, and that leads to collisions among these segments [30]. For the current study, the two models that completed the IK analysis were named scaled-generic model 3 (SGM3) and scaled-generic model 5 (SGM5). They are also mentioned as geometrically scaled models.

2.2. ***Scaling procedure: Modenese's algorithm for scaling optimal fiber and tendon slack length in geometrically scaled models.***

The scaling approach developed by Modenese exploited the insight provided by Zajac of the dimensionless Hill's muscle model [32]. We calculated the length of the MTUs (L^{mt}) using the definition of muscle length by Hill (Eq. 1, [33]), which depends on its tendon (l_t) and muscle fiber length (l_m), and its pennation angle (α):

$$L_m^{mt} = l_m * \cos\alpha + l_t \tag{1}$$

Introducing normalized variables ($l^{m,norm}$ and $l^{t,norm}$), Zajac (Eq. 2, [32]) showed the dependence between the L_m^{mt} and its OFL (l_o^m) and TSL ($l_{s,m}^t$). We employed the following equation (in vector notation) to estimate (l_o^m) and ($l_{s,m}^t$) for the SGMs:

$$L_m^{mt} = (l_{m,norm} * \cos\alpha) * l_o^m + l_{t,norm} * l_{s,m}^t \tag{2}$$

Based on the principles of the model by Hill, the $l_{m,norm}$ and $l_{t,norm}$ remain the same for a specific muscle in any individual. Then, the operating behavior of the muscles in a generic model (whose parameters, extracted from a cadaver, are phyisiologically valid) must be preserved when this model is geometrically scaled [22, 21]. Consequently, Modenese developed an optimization algorithm which solved Eq. 2, finding the values for OFL and TSL (for the new L_m^{mt}) to better preserve $l_{m,norm}$ and $l_{t,norm}$ as in the generic model (GM).

Modenese's algorithm contained three approaches that we modified so that they could be applied to every MTU *'m'* in the DSEM. The collection

of the N samples of the variables in Eq. 4, 5, and 6 is addressed in the coming section (2.3 *Scaling Procotol for the DSEM*). N is the optimal number of sampling points (being *'n'* each of those sampling point) that maximized the accuracy of the three scaling approaches (Eq. 3, [22]). N depends logaritmically on the Degrees of Freedom (DOF) operated by the muscle (or MTU) being analyzed.

$$N = 10^{DOF} \tag{3}$$

- **Linear approach:** We employed MATLAB to find a solution to the least square problem of calculating l_o^m and $l_{s,m}^t$ in Eq. 2. MATLAB did so while minimizing the error introduced by the pseudoinverse of a matrix (Eq. 4). If any of the new OFL or TSL are negative, they kept their original values from the GM.

$$\begin{bmatrix} l_o^{m,subj} \\ l_{s,m}^{t,subj} \end{bmatrix} = \begin{bmatrix} l_{1,norm}^{m,ref} * \cos\alpha_{m,1}^{ref} & l_{m,1,norm}^{t,ref} \\ \vdots & \vdots \\ l_{n,norm}^{m,ref} * \cos\alpha_{m,n}^{ref} & l_{m,n,norm}^{t,ref} \end{bmatrix}^{-1} * \begin{bmatrix} L_{m,1}^{mt,subj} \\ \vdots \\ L_{m,n}^{mt,subj} \end{bmatrix} + e \tag{4}$$

- **Constrained approach:** In this case, we used MATLAB's function *'lsqnonneg'* to find a solution to the least square problem of calculating l_o^m and $l_{s,m}^t$ in Eq. 2. The algorithm minimizes the error introduced by the pseudoinvserse while taking into account the restriction that the solution should be greater than zero. The constrained method showed a higher residue than the linear one due to the constraint introduced.

- **2-step approach:** This time OFL and TSL were calculated separately to ensure both were greater than zero.

    1. We scaled the TSL in the SGMs proportionally ($l_{s,m}^{t,prop}$) to the new MTU length ($L_m^{mt,subj}$). This adjustment kept the fraction of length represented by the TSL as in the GM (Eq. 5).

$$l_{s,m}^{t,prop} = \frac{l_{s,m}^{t,ref}}{L_m^{mt,ref}} * L_m^{mt,subj} \tag{5}$$

2. Calculation of the OFL using the linear approach and the proportional TSL ($l_{s,m}^{t,prop}$, Eq. 6).

$$l_o^{m,subj} = \begin{bmatrix} l_{1,norm}^{m,ref} * \cos\alpha_{m,1}^{ref} \\ \vdots \\ l_{n,norm}^{m,ref} * \cos\alpha_{m,n}^{ref} \end{bmatrix}^{-1} * \begin{bmatrix} L_{m,1}^{mt,subj} - l_{m,1}^{t,prop} \\ \vdots \\ L_{m,n}^{mt,subj} - l_{m,n}^{t,prop} \end{bmatrix} + e \quad (6)$$

3. Recalculation of the final value for TSL using the new value for OFL.

2.3. ***Scaling Protocol for the DSEM.***

Preserving the $l_{m,norm}$, and $l_{t,norm}$ of every muscle as in the GM required mapping these variables in the first place. For that purpose, we needed to explore the complete length excursion of all the MTUs in the DSEM. The length of a MTU only changes with the motion of the joints actuated by that specific MTU. Therefore, a complete mapping of the length's excursion of the biceps, for instance, implied exploring the whole ROM of the joints crossed by this muscle.

1. Identification of joints actuated by a certain MTU: Firstly, we calculated the muscle path (Eq. 7). We did so by computing the Eculidean distance from the origin of the MTU to its insertion in the initial step of the simulation *'n = 1'*. The joints actuated by a MTU were those crossed by its muscle path and θ is the joint angle in each step (*'n'*) of the simulation:

$$L_{m,n}^{mt}(\theta) = dist\left(insertion\ Node_{m,n}(\theta)\ ,\ \ origin\ Node_{m,n}(\theta)\right) \quad (7)$$

We also employed this formula (Eq. 7) to map the length of the MTUs in both, the GM ($L_{m,n}^{mt,ref}$) and the SGMs ($L_{m,n}^{mt,subj}$). For MTUs wrapping around bony contours, we followed the recommendations issued by [30] for *'Curved-Truss'* elements. From these measurements of L_m^{mt} we derived l_m and l_t using Eq. 1.

2. Several simulations were run with the GM to explore the ROM of the crossed joints. For every sampling point *'n'*, we calculated $\alpha^{ref}_{m,n}$ (Eq. 8), $l^{ref}_{m,n,norm}$ (Eq. 9), and $l^{ref}_{t,n,norm}$ (Eq. 10). We needed these parameters in order to solve Equation 2. In Eq. 8, $\alpha^{ref}_{m,1}$ stands for the pennation angle in the initial step of the simulation $n = 1$:

$$\alpha^{ref}_{m,n} = \arcsin\left(\frac{l^{m,ref}_{o} * \sin\alpha^{ref}_{m,0}}{l^{ref}_{m,n}}\right) \tag{8}$$

$$l^{ref}_{m,n,norm} = \frac{l^{ref}_{m,n}}{l^{m,ref}_{o}} \tag{9}$$

$$l^{ref}_{t,n,norm} = \frac{l^{ref}_{t,n}}{l^{t,ref}_{s}} \tag{10}$$

   - Values of $l^{ref}_{m,n,norm}$ over 1.5 or under 0.5 were filtered out since they are considered to be out of physiological conditions.
   - Values for $\alpha^{ref}_{m,n}$ over 0.84 rad were filtered out since they are considered to be out of physiological conditions.

3. We repeated step number 1 of this protocol, this time using the SGMs to map the lengths of the scaled MTU ($L^{mt,subj}_{m,n}$) in the same joint configurations.

4. Finally, we introduced the $L^{mt,subj}_{m}$, α^{ref}_{m}, $l^{ref}_{m,norm}$, and $l^{ref}_{t,norm}$, vectors into Eq. 2. Then, we applied the three solving techniques to find three sets of solutions (OFL and TSL) for every MTU *'m'*.

The new scaled models whose muscle parameters had been estimated by each of the three approaches proposed by Modenese were grouped under the names: scaled model 3 (SM3) and scaled model 5 (SM5). For example, the 'constrained SM3' refers to the SM3 whose muscle parameters have been modified using the constrained approach.

2.4. ***Motion Data.***

We used Range Of Motion (ROM) trials [2] in order to map the length excursion of every MTU in the DSEM, apart from other variables, as we introduced in the protocol introduced in the previous section.

Then, we conducted two sets of trials to evaluate the effects on consistency of adjusting OFL and TSL in the DSEM. We selected two movements from Bolsterlee's dynamic tests [14]. The two dynamic tests chosen were: forward shoulder flexion and scaption. We considered the first one to be an uncomplicated movement since it simply involved the motion of the shoulder on a single plane. However, the scapular retraction (scaption) included multiple and simultaneous rotations plus the scapula covering the extremes of its ROM, which is usually troublesome. Secondly, the force trials selected to examine the variation in muscle force production included: shoulder forward flexion (we called it anteflexion to distinguish this one from the dynamic test) and abduction. We decided to carry these two test to reproduce the conditions of Wu's investigation [28], since we employed his results for the validation of muscle forces.

2.5. ***Evaluation of the scaling protocol and each of the three scaling approaches consequences on consistency and muscle force production.***

For the evaluation of the consistency of the models, we followed the guidelines established by Winby [21]. He recommended calculating the MMSE of the $l_{m,norm}$ between the reference (GM) and each of the scaled models (SGMs and SMs). The MMSE is the average RMSE of the $l_{m,norm}$ of all the muscles in the scaled models throughout the two dynamic tests. The lower the MMSE of a certain model is, the higher its consistency. Therefore, the scaling approach providing the most substantial improvement in the consistency compared with the SGMs (which we hypothesized that would be the least consistent models), would be that one yielding the lowest MMSE. Besides that, we also checked whether if the scaling approaches improved the working region of the muscles in the SGMs. In doing so, we compared the proportion of the total humeral elevation ROM that out-of-range muscles operated under physiological conditions before and after muscle parameter scaling. Out-of-range muscles are those muscles which spent more than one step of

the simulation working out of the physiological area in the F-L curve (Fig. 1). If a particular MTU worked within bounds throughout the entire ROM, it received a value of 1.

Improving the working region of the muscles had consequences into their muscle force generation ability. We compared the difference in force production of four rotator cuff muscles in the SGMs and the SMs. In his investigation, Wu [28] also scaled an upper-limb model [17] in Opensim using Modenese's algorithm. Therefore, we expected to obtain similar variations in muscle forces.

3. Results

The protocol employed in the current research to scale OFL and TSL delivered physiologically feasible values [34, 28]. Table 1 contains the differences in the length of the segments (clavicle, humerus, and radius) and muscle parameters in the SMs compared to the GM. Values over or below one means that the segment or parameter is longer or shorter than in the GM, respectively.

	Subject 3	Subject 5
Length of clavicle	0.89	1.05
Length of humerus	0.93	0.97
Length of radius	0.95	1.02
Total	**0.92**	**1.013**
Optimal Fiber Length (avg)	0.9502	1.085
Tendon Slack Length (avg)	1.0491	1.035

Table 1: Variations in length of the model segments (due to geometrical scaling) and of muscle parameters (constrained approach). These values are expressed as ratios between the length in the SM and the GM. (e.g., $l^{subj}_{clav}/l^{ref}_{clav}$). Therefore, if the length of the clavicle in SM3 is 0.89, $l^{subj}_{clav} = 0.89 * l^{ref}_{clav}$. The row named "Total" contains the averaged value of the three segments. For the OFLs and TSLs, the ratios are the average of the 31 muscles in the DSEM.

The constrained approach delivered muscle parameters which did not follow the variation in the segments' length of either of the two SMs. For subject

5 (S5), scaling increased the length of both, muscle parameters and model segments, although not in the same proportion. While OFLs and TSLs were elongated 8'5% and 3.5%, the bones of SM5 were just 1.3% longer than in the GM. Furthermore, in subject 3 (S3), not only did the muscle parameters not decrease proportionally to the segments, but the TSLs increased 4.91% on average.

3.1. ***Consistency of the Scaled models.***

Figure 2 shows the normalized length excursions of the scapular section of the deltoid during the scaption trial. This muscle operated out of range (below 0.5 $l_{m,norm}$, Fig 2) from 30º in SGM3 (dashed red line) and 60º in SGM5 (dashed green line) until the end of the trial and 70º respectively.

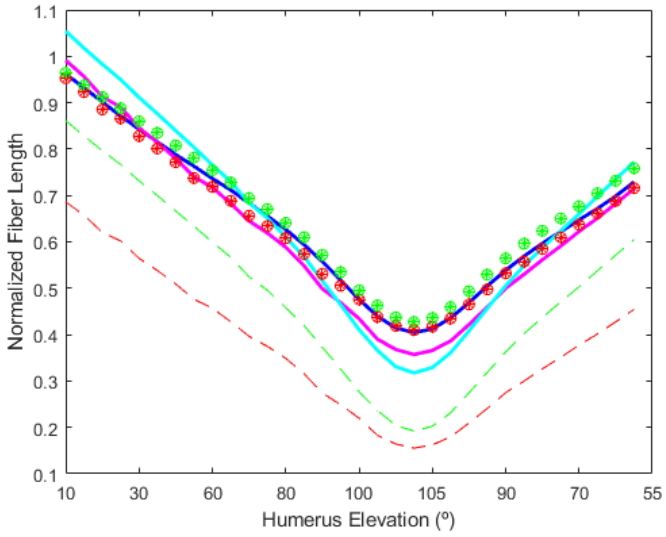

Figure 2: **Variations in the length excursion of the scapular section of the deltoid (one of the muscles working out of range in the SGMs) throughout the scaption trial of Subject 3**. In blue, the normalized length excursion of the muscle in the GM (reference model). The dashed lines depict the deviation in SGM3 (red) and SGM5 (green) due to geometrical scaling. The circles represent the length excursion in SM3 (red) and SM5 (green) after having their parameters scaled with the constrained approach. The linear technique delivered identical results (star marks) in SM3 (red) and SM5 (green). Finally, the solid lines in magenta (SM3) and cyan (SM5) illustrate the excursion of the fibers after scaling the muscle parameters using the 2-step approach.

The constrained (circles mark) and linear (stars mark) adjustment of muscle parameters provided the best fit with the GM (solid blue line). The same remark holds for all the muscles that actuated out of bounds in the SGMs, like the deltoid.

The median of the out-of-range muscles in SGM3 was 0.26 (Fig 3). The constrained estimation of l_o^m and l_s^t, brought that number down to 0.027. The other two approaches also achieved substantial reductions in MMSE for out-of-range muscles. The 2-step scaling lowered the MMSE from 0.21 in SGM3 and 0.23 in SGM5 to 0.034 and 0.096, respectively. The linear approach decreased those values to 0.08 and 0.068. The most considerable reduction was achieved by the constrained technique, which yielded a 0.028 and 0.046 MMSE for SM3 and SM5 (in red in Table 2).

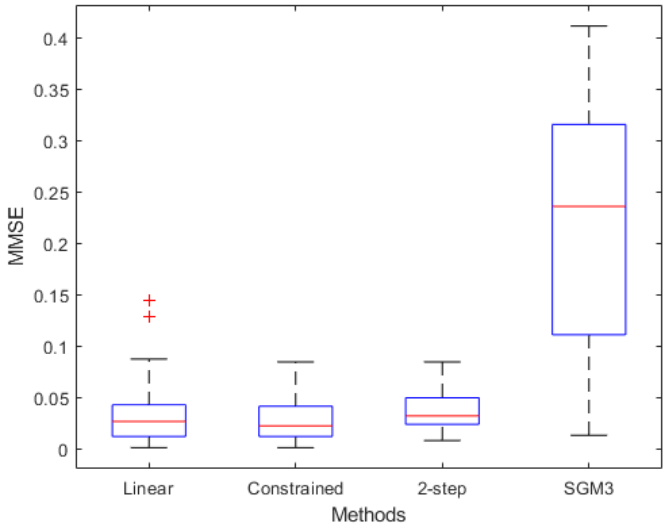

Figure 3: Level of consistency delivered by geometrical scaling (SGM3) and muscle parameter scaling (Linear, Constrained and 2-step). The lowest the MMSE, the highest the consistency. The MMSE is the averaged RMSE of all the muscles out of range (Appendix A) during the dynamic trials of Subject 3. The red line in the boxplots indicates the median, meaning that half of the muscles in the DSEM showed MMSEs lower than this value. The upper and lower sides of the boxplots represent the 25th and 75th percentile. These percentiles indicate that one quarter and three quarters, respectively, of the muscles in the DSEM showed lower MMSEs. The cross markers illustrate the outliers.

	Subject 3				Subject 5			
	lin	cns	2stp	SGM	lin	cns	2stp	SGM
OR Musc	0.038	0.028	0.034	0.21	0.068	0.046	0.096	0.23
WR Musc	0.03	0.029	0.03	0.11	0.038	0.031	0.044	0.112
All Musc	0.03	0.029	0.03	0.127	0.043	0.03	0.053	0.14

Table 2: MMSE of the thirty-one muscles in the DSEM throughout the two dynamic trials ('All Musc'). For more information about the relation between MMSE and consistency refer to Fig. 3. Each column correspond to each of the three scaling approaches (lin = linear, cns = constrained, 2stp = 2-step). The column labelled 'SGM' contains the MMSE of the geometrically scaled models (SGM). In red ('OR Musc'), the averaged results taking into account only muscles operating out of range (Appendix A). In green ('WR Musc'), the results from muscles operating within physiological range.

Figure 4 displays the pectoralis major's length excursions throughout the flexion trial. For muscles that operated under physiological conditions (pectoralis major among them), the reductions delivered by the three approaches were not as remarkable as for muscles out of range (Fig. 3 and Fig. 5). The median of the MMSE of fibers actuating within bounds was 0.085 already for the SGM5 (SGM5 in Fig 5). However, the constrained method managed to lower that value to 0.019. This technique achieved the most significant reductions again, decreasing the MMSE from 0.11 and 0.112 to 0.029 and 0.028 for SM3 and SM5, respectively (in green in Table 2).

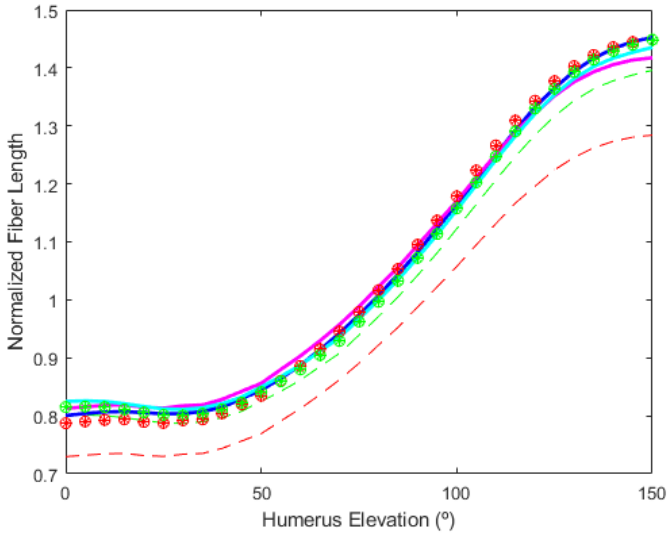

Figure 4: **Variations in the length excursion of the pectoralis major (one of the muscles working under physiological conditions in the SGMs) throughout the forward flexion trial of Subject 5**. For more information about the lines and markers in the figure, refer to Fig. 2

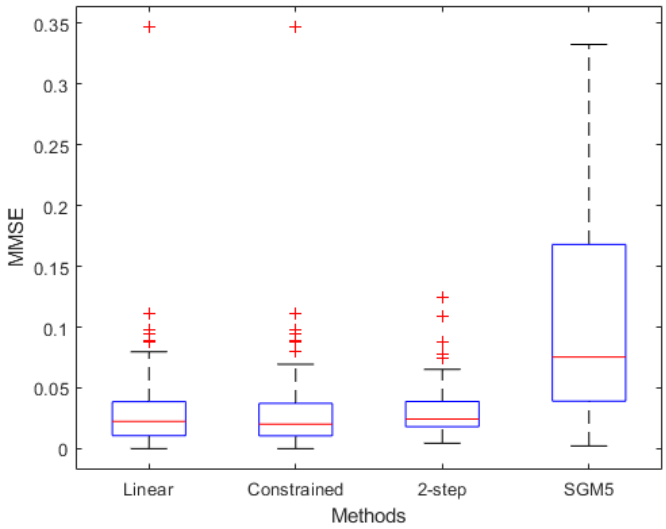

Figure 5: Level of consistency delivered by geometrical scaling (SGM5) and muscle parameter scaling (Linear, Constrained, 2-step). The lowest the MMSE, the highest the consistency. The MMSE is the averaged RMSE of all the muscles within range during the dynamic trials of Subject 5. For more information about the figure, refer to Fig. 3

Figures 6 and 7 illustrate the working range of the muscles actuating out of bounds in the SGMs throughout the dynamic trials. The Y-axis incorporates the twenty-two muscles operating out of range in SGM3 (Fig. 6) and SGM5 (Fig. 7). The dark blue regions depict the working area of these muscles in the SGMs. The green zones represent the improvements delivered by the constrained approach. Constrained scaling of l_o^m and l_s^t brought every muscle to work under physiological conditions but for the serratus anterior in Figure 6. It even achieved that out-of-range muscles operated within bounds for a higher percentage of the humeral ROM in the SMs than in the GM (in green in Table 3).

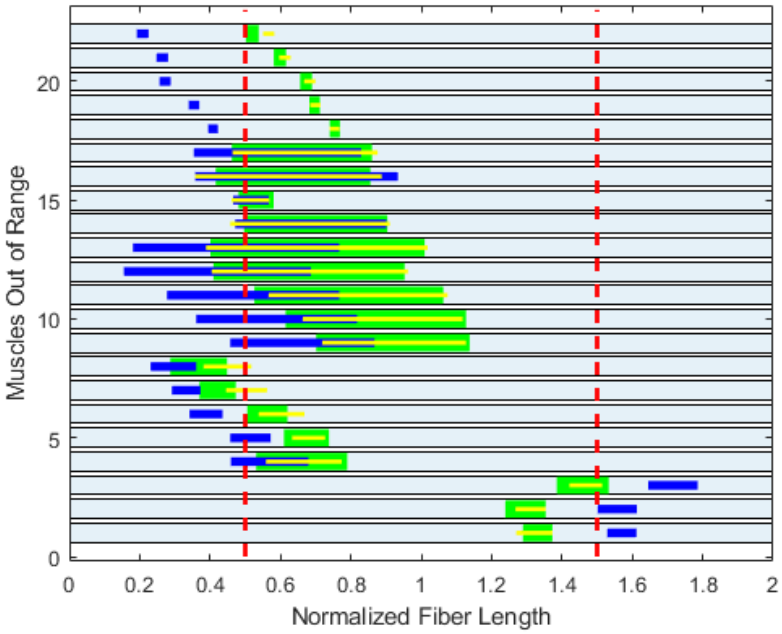

Figure 6: Shifts in the working region of out-of-range muscles in S3 caused by scaling OFL and TSL (constrained approach). The blue area depicts the operating range of muscles out of range (outside of the zone defined by the red dashed lines) in SGM3 due to geometrical scaling (e.g., teres minor and triceps). The yellow lines show the operating region of the same set of muscles in the GM (reference model), which should be preserved after geometrical modifications according to Winby [21]. The green regions represent the improvement in the working area after scaling OFL and TSL with the constrained approach. Therefore, muscles in which the green and yellow regions overlap, are appropriately scaled (e.g., scapular and clavicular part of the deltoides). The name of the twenty-two muscles displayed on the Y-axis are specified in Appendix A, table A.6.

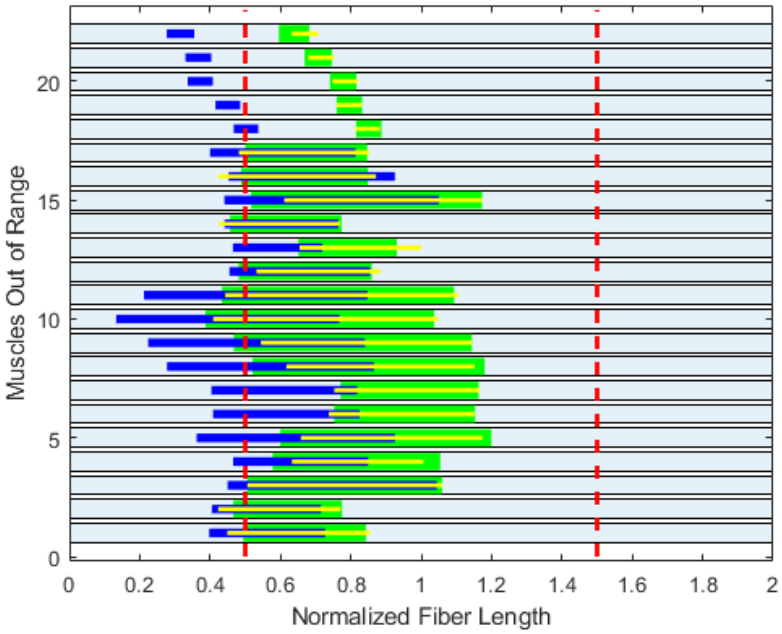

Figure 7: Shifts in the working region of out-of-range muscles in S5 caused by scaling OFL and TSL (constrained approach). Muscles in which the green and yellow regions overlap, are appropriately scaled (e.g., pectoralis minor and serratus anterior). The name of the twenty-two muscles displayed on the Y-axis are specified in Appendix A, table A.7. For more information about the figure and the consequences of muscle parameter scaling on their working area, refer to Fig. 6.

	OR Musc				**All Musc**			
	lin	cns	2stp	SGM	lin	cns	2stp	SGM
S3	0.9	0.92	0.88	0.59	0.97	0.98	0.98	0.91
S5	0.93	0.94	0.9	0.66	0.96	0.98	0.98	0.93
GM	0.9				0.9805			

Table 3: Averaged proportion (out of 1, being 1 the whole ROM) of the humeral elevation ROM that muscles spent working within the physiological conditions. In 'Musc. OR', the values for muscles working out of range for longer than one step of the simulation. In 'All musc', the results taking into account the thirty-one MTUs in the DSEM. The color code is the same as in Fig. 6 and 7. The information contained in the colored rows and columns together with the mentioned figures illustrate the improvement in the working area of the muscles delivered by muscle parameter scaling. For more information about the columns and rows' labels, refer to Table 2.

The 2-step approach outperformed the constrained method for muscles whose TSL is zero in the SGM (Appendix B and Fig. 8). In this case, both linear and constrained scaling delivered higher MMSE values than geometrical scaling. The 2-step technique was the only one reducing the MMSE compared to the SGM (Fig 9 and highlighted in green in Table 4).

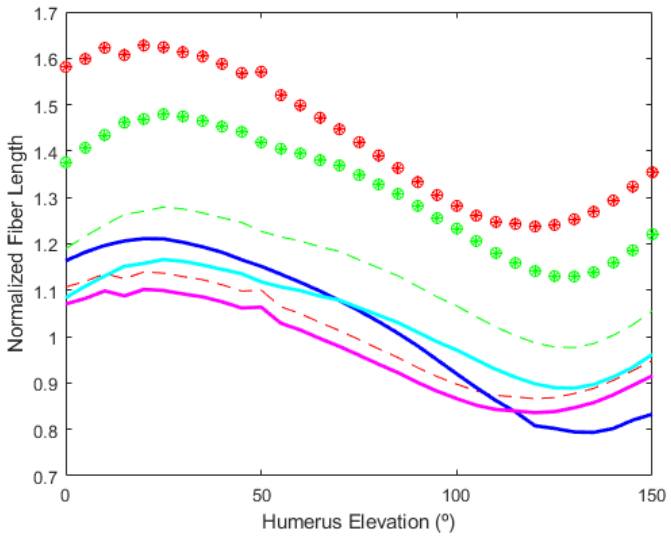

Figure 8: **Variations in the length excursion of the serratus anterior (one of the muscles whose original tendon slack length is zero) throughout the forward flexion trial of Subject 5**. For more information about the graphic, refer to Fig. 2

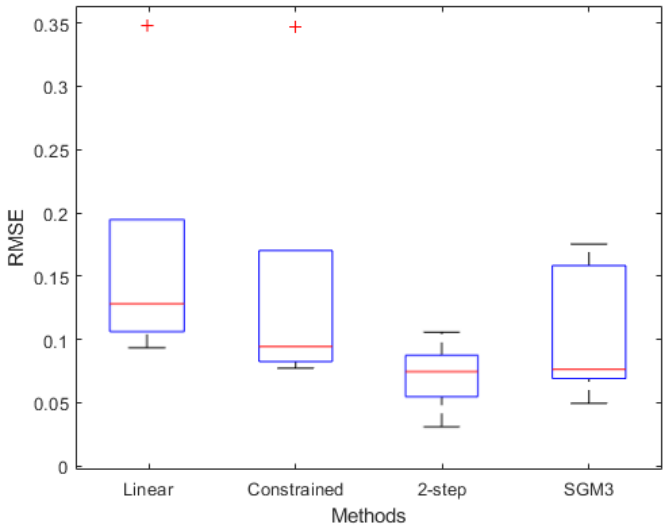

Figure 9: Level of consistency delivered by geometrical scaling (SGM3) and muscle parameter scaling (Linear, Constrained, 2-step). The lowest the MMSE, the highest the consistency. Only muscles whose original TSL was zero (Appendix B) in the GM are considered for this graphic. For more information about the boxplots, refer to Fig. 3.

	Linear	Constrained	2-step	SGM
S3	0.175	0.145	0.06	0.105
S5	0.155	0.109	0.077	0.079

Table 4: MMSE of the muscles whose original TSL is zero (Appendix B) throughout the two dynamic trials for both subjects 3 and 5. In green, the only values lower than the MMSEs in the SGMs, corresponding to the 2-step approach. For more information about the relation between MMSE and consistency refer to Fig.3.

3.2. ***Consequences on muscle force production.***

The averaged forces of five of the rotator cuff muscles (clavicular and scapular deltoid, supraspinatus, infraspinatus, subscapularis, and teres minor) are shown in Table 5. There were three muscles whose variation in the force generation did not match the results from Wu's research: the supraspinatus, and subscapularis in SM3 and the infraspinatus in SM5 (in red in Table 5). The teres minor was the muscle that experienced the most substantial increase in force production due to constrained scaling.

	Subject 3	**Subject 5**	**Reference [28]**
Deltoid	-3.17 %BW	-3.88 %BW	-1.75 %BW
Infraspinatus	-0.36 %BW	3.61 %BW	- 4.21 %BW
Supraspinatus	27.73 %BW	-2.8 %BW	-1.27 %BW
Subscapularis	7.12 %BW	-4.29 %BW	-4.19 %BW
Teres Minor	-19.78 %BW	-15.75 %BW	-
Total Musc Force	**-1.1 %BW**	**-1.2 %BW**	**- 1.9 %BW**

Table 5: Differences in force production (expressed as the percentage of the Body Weight of the subject) before and after scaling OFL and TSL using the constrained approach in five rotator cuff muscles. A positive value means that the force generated by a muscle is larger in the SGM than in the SM. Conversely, a negative value implies that the force in the SGM is smaller than in the SM. The reference column shows the difference in muscle force production from a study using the same scaling technique [28]. In red, the muscle forces that did not follow the variation (after muscle parameter scaling) observed in Wu's publication. Although the reference study did not consider the Teres Minor, we included it on this table because it is the muscle experiencing the largest increase in force production. The last row indicates the averaged variation in force generation of the thirty-one MTUs in the SMs.

4. Discussion

We hypothesized that adjusting OFL and TSL in geometrically scaled models will improve their consistency. Our results have shown that the three scaling approaches broadly achieve that. Constrained, linear, and 2-step scaling of muscle parameters, in that specific order, deliver the lowest MMSE values (Fig. 3 and 5). That means, they provide the highest consistencies compared to geometrically scaled models.

The constrained approach yields MMSEs as low as 0.029 for SM3 (Table 2). That indicates that the muscles in SM3 show a behavior 97.1% similar to the GM, despite the geometrical modifications. Therefore, a particular muscle reaches its maximal force at the same humeral elevation angle with a 2.9% error in the SM3 as in the GM (Figure 1). For that reason, there is only a 2.9% loss in consistency in SM3 with respect to GM3. Furthermore, muscle parameter constrained adjustment preserves the extent of the humeral elevation ROM in which muscles work under physiological conditions in the SMs (0.98) in the same level as in the GM (0.9805, Table 3). Avoiding the reduction of this ratio implies that the force generation capability of the model

does not diminish, regardless of geometrically scaling.

The consistency analysis of the SGMs (whose muscle parameters are not adjusted) provides very different results. Firstly, the MMSE values in the SGMs are 78% higher than in the SMs (Table 2). That implies that SGMs are 78% less consistent than SMs. In other words, not adjusting OFL and TSL after geometrically scaling the DSEM causes a significant loss on consistency. Secondly, geometrical scaling brought twenty-two muscles to operate outside the physiological fiber length range (Fig. 6 and 7, and Appendix A). They work as much as 41% of the humeral elevation ROM out of range (Table 3, SGM3). During that extent, their force production capacity is limited to 1% of their maximum force [30], restricting the force production of the whole model. Consequently, the load sharing algorithm of the DSEM may fail to find a solution for the distribution of muscle forces [19]. Nevertheless, adjusting their OFLs and TSLs to the new MTU lengths reduces the MMSEs as much as 84% (in red in Table 2). Moreover, the adjustment brings these muscles back to work within range for at least 92% of the humeral elevation (in green in Table 3).

Therefore, geometrically-scaled models are inconsistent, and inconsistent models are unreliable since the behavior of their muscles is altered compared with the reference model, the GM (in which they exhibit their theoretically correct behavior). This is due to differences in its operating region and fiber length excursion caused by geometrical scaling. We have demonstrated that such inconsistencies are fixed by adjusting OFL and TSL to the scaled MTUs length. **In consequence, we acknowledge that the results endorse our first hypothesis. Adjusting OFL and TSL in geometrically scaled upper-limb models improves their consistency.**

Scaling OFL and TSL provokes an increase in the muscle force capacity of the models as well. Muscles such as the Teres Minor, whose three contractile elements were out of range in the SGMs (elements from eighteen to twenty in Figures 6 and 7), experience the most considerable increase in force generation (Table 5). Tuning the OFLs and TSLs of those three elements allows them to work under physiological conditions. Therefore, the 1% restriction on their maximal force ceases, and their force production increases. The same reasoning applies for any of the muscles that were working out of range in the SGMs and that, thanks to scaling their muscle parameters, are

back to operating under physiological conditions. **Scaling OFL and TSL produces an increase in muscle force production. Not only muscle parameters must be adjusted to preserve consistency, but also to avoid the reduction in the force generation due to geometrical scaling.** Accordingly, SGMs show lower force generation capacity than SMs (Table 5). Although producing consistent scaled models is an important step in the quest to represent the muscle capacity of a subject, further research is needed to evaluate the influence of other muscle parameters in the generation of force, such as the PCSA.

To the best of our knowledge, this is the first study evaluating the effect of scaling OFL and TSL on consistency in upper-limb models. Validating the presented results is thus a challenging task. The only solution plausible is comparing our MMSEs to those from an article employing a lower-limb model [22]. Even though our MMSEs are slightly higher, they are consistent in magnitude (0.029 and 0.03, Table 2) with the values shown in Modenese's study (maximal MMSE of 0.019). Likewise, our correlations are not as high (0.99), but they are above 0.95 (Appendix C, Tables C.8 and C.9). Consequently, we can ratify that the consistency levels reached in our study are almost identical to those in Modenese's paper [35].

The new values for OFLs and TSLs fall within range with data from corpses of similar dimensions to S3 and S5 [28, 34]. Hence, we guarantee that the muscle parameters delivered by the constrained approach are physiologically valid. The literature on the topic suggests that bone dimensions and muscle parameter scaling hold a non-linear relation [29, 8]. The results presented in this study support that statement as well (Table 1).

The constrained approach struggles, however, with muscles whose original TSL is zero. It even weakens their consistency and those fibers show lower MMSEs in the SGMs than in the constrained SMs. The 2-step technique, by contrast, delivers the smallest MMSEs in this situation (Figure 9 and in green in Table 4) and thus, the highest consistency. The non-varying tendons in our model may be the reason for the poor performance of the linear and constrained approaches. Modenese has stated that his algorithm struggles to estimate the OFL and TSL in muscles "*...whose tendon length does not stretch significantly*" [22]. Tendons in the DSEM are stiff elements, meaning they do not stretch at all [30]. Additionally, for muscles whose original TSL

is zero (Appendix B), the linear and constrained techniques find solving Eq. 4 truly challenging. Probably, our MMSEs and correlations values are not as ideal as in Modenese's article due to the stiff tendons in the DSEM as well.

Wu's investigation [28] allows us to validate the muscle force variation. We have compared the differences in forces of four rotator cuff muscles before and after scaling OFL and TSL. Although most of those muscles show a similar increase in force generation, three of them do not follow that fashion (in red in Table 5). The subscapularis, supraspinatus (S3) and infraspinatus (S5) produce larger forces in the SGMs than in the SMs. This discrepancy may be due to different load-sharing algorithms. Wu's model distributes the net joint moments "*...proportionally among synergistic muscles*" [17]. Conversely, the DSEM load-sharing algorithm distributes the muscle forces to minimize the energy expenditure [19]. The difference in this criterion may be the cause of the discrepancy in the force difference in the rotator cuff muscles. Nevertheless, both studies agree on the increase in the total muscle force production in SMs with respect to SGMs (Table 5).

The scaling algorithm employed in this study introduces two limitations. In the first place, it has not been demonstrated that the normalized fiber length excursion and the force-angle relation (Figure 1) are the same in different people. Secondly, Modenese's algorithm regards the working ranges of the muscles in the reference model (GM) as representative of a healthy individual. However, our generic model was created using data from a cadaver. In consequence, the scaling protocol in this paper should be used carefully with samples such as elite athletes.

The sample (two subjects) of this investigation is too reduced for the results to be representative. We therefore recommend repeating the current study with a larger sample. Furthermore, a future study could include Maximal Voluntary Contraction (MVC) tests. We have assessed the effects of muscle parameter scaling in the muscle force production for dynamic tests, but the impact on MVCs is still unknown.

Lastly, the validation performed is limited. We only found three articles about scaling muscle parameters in upper-limb models [27, 28, 14], and none of them evaluated the effects on consistency. Since the literature on the topic is scarce, alternative validation techniques should be considered. Applying

the scaling protocol contained in this article to Nikooyan geometrically scaled models represents a reliable option [19]. In this way, the estimated contact forces could be compared with experimental data from instrumented endoprostheses.

5. Conclusion

- Any research which intends to modify the geometrical parameters of the DSEM (or any other upper-limb MSK model) must adjust the OFL and TSL accordingly, in order to preserve the consistency and muscles behavior in the scaled version. Inconsistent models are unreliable and not capable of representing the muscle force capacity of the scaled subject.

- Scaled versions of the DSEM whose OFLs and TSLs have been adjusted are 78% more consistent and their MTUs produce up to 1.2 %BW larger forces than geometrically scaled versions.

- The scaling protocol contained in this paper delivers losses in consistency lower than 5%. Furthermore, it does not require other experimental data than ROM recordings and it is computationally inexpensive.

Appendix A. List of muscles working out of range.

The following tables contain the names of the muscles actuating out of range displayed on Figure 6 for Subject 3 and Figure 7 for Subject 5. These are also the muscles labeled as 'OR Musc' or out-of-range muscles in Tables 2 and 3.

Nr. in Fig. 6	Name of the muscle
1, 2, 3	Trapezius Scapular Part
4	Pectoralis Minor
5, 6, 7, 8	Serratus Anterior
9, 10, 11, 12, 13	Deltoides Scapular Part
14	Deltoides Clavicular Part
15	Infraspinatus
16,17	Subscapularis
18, 19, 20	Teres Minor
21, 22	Triceps lateral part

Table A.6: Name of the muscles corresponding to the numbers shown on the Y-axis in Figure 6.

Nr. in Fig. 7	Name of the muscle
1, 2, 3	Trapezius Scapular Part
4, 5	Pectoralis Minor
6, 7	Serratus Anterior
8, 9, 10, 11	Deltoides Scapular Part
12, 13	Deltoides Clavicular Part
14	Infraspinatus
15, 16, 17	Subscapularis
18, 19, 20	Teres Minor
21, 22	Triceps lateral part

Table A.7: Name of the muscles corresponding to the numbers shown on the Y-axis in Figure 7.

Appendix B. List of muscles whose original Tendon Slack Length is zero in the DSEM.

The muscle fibers whose Tendon Slack Length (TSL) is zero in the reference model (generic version of the DSEM) are: four elements of the Serratus Anterior and one element of the Subscapularis.

Appendix C. Correlation values.

We calculated the correlation coefficients between the fiber length excursion in the scaled models and the GM (reference model) to evaluate the

similarity of their curves (such as the curves displayed on Fig 2, 4, and 8). We compared these values to the correlation coefficients from Modenese's publication [22].

	Max	Min	Mean
SM3	1	0.3	0.97
SM5	1	0.15	0.95

Table C.8: Correlation coefficients of the scaption test for SM3 and SM5. Several muscles show a correlation of 1 (maximal value) but the minimal correlation corresponds to the brachioradialis and the serratus anterior in SM3 and SM5 respectively. The mean value is the averaged correlation coefficient of all the muscles in the DSEM.

	Max	Min	Mean
S3	1	0.45	0.98
S5	1	0.14	0.97

Table C.9: Correlation coefficients of the flexion test for SM3 and SM5. Several muscles show a correlation of 1 (maximal value) but the minimal correlation corresponds to the serratus anterior and the subscapularis in SM3 and SM5 respectively. The mean value is the averaged correlation coefficient of all the muscles in the DSEM.

References

[1] H. Veeger, F. van der Helm, Shoulder function: The perfect compromise between mobility and stability, Journal of Biomechanics 40 (2007) 2119–2129.

[2] D. Magermans, E. Chadwick, H. Veeger, F. van der Helm, Requirements for upper extremity motions during activities of daily living, Clinical Biomechanics 20 (2005) 591–599.

[3] F. van der Helm, H. Veeger, Quasi-static analysis of muscle forces in the shoulder mechanism during wheelchair propulsion, Journal of Biomechanics 29 (1996) 39–52.

[4] F. Steenbrink, J. de Groot, H. Veeger, F. van der Helm, P. Rozing, Glenohumeral stability in simulated rotator cuff tears, Journal of Biomechanics 42 (2009) 1740–1745.

[5] H. Kainz, M. Wesseling, L. Pitto, A. Falisse, S. Van Rossom, A. Van Campenhout, F. De Groote, K. Desloovere, C. Carty, I. Jonkers, O 107 - Impact of subject-specific musculoskeletal geometry on estimated joint kinematics, joint kinetics and muscle forces in typically developing children., Gait & posture 65 Suppl 1 (2018) 223–225.

[6] M. Wesseling, F. De Groote, C. Meyer, K. Corten, J.-P. Simon, K. Desloovere, I. Jonkers, Subject-specific musculoskeletal modelling in patients before and after total hip arthroplasty, Computer Methods in Biomechanics and Biomedical Engineering 19 (2016) 1683–1691.

[7] T. A. Correa, R. Baker, H. Kerr Graham, M. G. Pandy, Accuracy of generic musculoskeletal models in predicting the functional roles of muscles in human gait, Journal of Biomechanics 44 (2011) 2096–2105.

[8] F. Heinen, M. E. Lund, J. Rasmussen, M. de Zee, Muscle–tendon unit scaling methods of Hill-type musculoskeletal models: An overview, Proceedings of the Institution of Mechanical Engineers, Part H: Journal of Engineering in Medicine 230 (2016) 976–984.

[9] B. Bolsterlee, D. H. E. J. Veeger, E. K. Chadwick, Clinical applications of musculoskeletal modelling for the shoulder and upper limb, Medical & Biological Engineering & Computing 51 (2013) 953–963.

[10] L. L. Menegaldo, L. F. de Oliveira, Effect of muscle model parameter scaling for isometric plantar flexion torque prediction, Journal of Biomechanics 42 (2009) 2597–2601.

[11] P. Gerus, M. Sartori, T. F. Besier, B. J. Fregly, S. L. Delp, S. A. Banks, M. G. Pandy, D. D. D'Lima, D. G. Lloyd, Subject-specific knee joint geometry improves predictions of medial tibiofemoral contact forces, Journal of Biomechanics 46 (2013) 2778–2786.

[12] R. Hainisch, M. Gfoehler, M. Zubayer-Ul-Karim, M. G. Pandy, Method for determining musculotendon parameters in subject-specific musculoskeletal models of children developed from MRI data, Multibody System Dynamics 28 (2012) 143–156.

[13] V. Carbone, R. Fluit, P. Pellikaan, M. van der Krogt, D. Janssen, M. Damsgaard, L. Vigneron, T. Feilkas, H. Koopman, N. Verdonschot,

TLEM 2.0 – A comprehensive musculoskeletal geometry dataset for subject-specific modeling of lower extremity, Journal of Biomechanics 48 (2015) 734–741.

[14] B. Bolsterlee, A. N. Vardy, F. C. van der Helm, H. (DirkJan) Veeger, The effect of scaling physiological cross-sectional area on musculoskeletal model predictions, Journal of Biomechanics 48 (2015) 1760–1768.

[15] C. Y. Scovil, J. L. Ronsky, Sensitivity of a Hill-based muscle model to perturbations in model parameters, Journal of Biomechanics 39 (2006) 2055–2063.

[16] D. C. Ackland, Y.-C. Lin, M. G. Pandy, Sensitivity of model predictions of muscle function to changes in moment arms and muscle–tendon properties: A Monte-Carlo analysis, Journal of Biomechanics 45 (2012) 1463–1471.

[17] S. L. Delp, F. C. Anderson, A. S. Arnold, P. Loan, A. Habib, C. T. John, E. Guendelman, D. G. Thelen, OpenSim: Open-source software to create and analyze dynamic simulations of movement, IEEE Transactions on Biomedical Engineering (2007).

[18] E. Passmore, A. Lai, M. Sangeux, A. G. Schache, M. G. Pandy, Application of ultrasound imaging to subject-specific modelling of the human musculoskeletal system, Meccanica 52 (2017) 665–676.

[19] A. Nikooyan, H. Veeger, P. Westerhoff, F. Graichen, G. Bergmann, F. van der Helm, Validation of the Delft Shoulder and Elbow Model using in-vivo glenohumeral joint contact forces, Journal of Biomechanics 43 (2010) 3007–3014.

[20] B. Goislard de Monsabert, G. Rao, A. Gay, E. Berton, L. Vigouroux, A scaling method to individualise muscle force capacities in musculoskeletal models of the hand and wrist using isometric strength measurements, Medical & Biological Engineering & Computing 55 (2017) 2227–2244.

[21] C. Winby, D. Lloyd, T. Kirk, Evaluation of different analytical methods for subject-specific scaling of musculotendon parameters, Journal of Biomechanics 41 (2008) 1682–1688.

[22] L. Modenese, E. Ceseracciu, M. Reggiani, D. G. Lloyd, Estimation of musculotendon parameters for scaled and subject specific musculoskeletal models using an optimization technique, Journal of Biomechanics 49 (2016) 141–148.

[23] A. Van Campen, G. Pipeleers, F. De Groote, I. Jonkers, J. De Schutter, A new method for estimating subject-specific muscle-tendon parameters of the knee joint actuators: a simulation study, International Journal for Numerical Methods in Biomedical Engineering 30 (2014) 969–987.

[24] Antoine Falisse, B. Department of Kinesiology, KU Leuven, Leuven, ; Sam Van Rossom ; Ilse Jonkers ; Friedl De Groote, EMG-Driven Optimal Estimation of Subject-SPECIFIC Hill Model Muscle–Tendon Parameters of the Knee Joint Actuators, IEEE Transactions on Biomedical Engineering 64 (2017) 2253–2262.

[25] M. Sartori, M. Reggiani, A. J. van den Bogert, D. G. Lloyd, Estimation of musculotendon kinematics in large musculoskeletal models using multidimensional B-splines, Journal of Biomechanics 45 (2012) 595–601.

[26] F. De Groote, A. Van Campen, I. Jonkers, J. De Schutter, Sensitivity of dynamic simulations of gait and dynamometer experiments to hill muscle model parameters of knee flexors and extensors, Journal of Biomechanics 43 (2010) 1876–1883.

[27] B. A. Garner, M. G. Pandy, Estimation of Musculotendon Properties in the Human Upper Limb, Annals of Biomedical Engineering 31 (2003) 207–220.

[28] W. Wu, P. V. Lee, A. L. Bryant, M. Galea, D. C. Ackland, Subject-specific musculoskeletal modeling in the evaluation of shoulder muscle and joint function, Journal of Biomechanics 49 (2016) 3626–3634.

[29] S. R. Ward, C. M. Eng, L. H. Smallwood, R. L. Lieber, Are Current Measurements of Lower Extremity Muscle Architecture Accurate?, Clinical Orthopaedics and Related Research 467 (2009) 1074–1082.

[30] F. van der Helm, A finite element musculoskeletal model of the shoulder mechanism, Journal of Biomechanics 27 (1994) 551–569.

[31] H. Veeger, The position of the rotation center of the glenohumeral joint, Journal of Biomechanics 33 (2000) 1711–1715.

[32] Felix E. Zajac and Jack M. Winters, Modeling Musculoskeletal Movement Systems: Joint and Body Segmental Dynamics, Musculoskeletal Actuation, and Neuromuscular Control, Biomechanics and Movement organization (1990).

[33] A. V. Hill, The Heat of Shortening and the Dynamic Constants of Muscle, Proceedings of the Royal Society B: Biological Sciences 126 (1938) 136–195.

[34] J. Langenderfer, S. A. Jerabek, V. B. Thangamani, J. E. Kuhn, R. E. Hughes, Musculoskeletal parameters of muscles crossing the shoulder and elbow and the effect of sarcomere length sample size on estimation of optimal muscle length, Clinical Biomechanics 19 (2004) 664–670.

[35] J. L. Hicks, T. K. Uchida, A. Seth, A. Rajagopal, S. L. Delp, Is My Model Good Enough? Best Practices for Verification and Validation of Musculoskeletal Models and Simulations of Movement, Journal of Biomechanical Engineering 137 (2015) 020905.